Rev.Adv.Mater.Sci. 5 (2003) 134-138

STRUCTURE AND PROPERTIES OF ELECTRODEPOSITED NANOCRYSTALLINE FCC Ni-Fe ALLOYS

F. Ebrahimi and H.Q. Li

Materials Science and Engineering Department, University of Florida, P.O. Box 116400, Gainesville, FL 32611, USA

Received: July 01, 2003

Abstract. Nanocrystalline Ni-Fe alloys with composition in the 5 wt% to 50 wt% Fe range were fabricated via the electrodeposition method. Very fine grain size (≈11nm) with nearly random crystallographic orientation was obtained in alloys with equal or more than 15 wt% Fe. For a nominally constant grain size, the hardness of the deposits decreased and the level of internal stresses increased with raising the iron content above 15 wt%. At low iron concentrations, the deposit showed large grain size with a strong <100> texture. These observations are discussed in terms of the development of the structure during the deposition process.

1. INTRODUCTION

During the past decade, extensive work on the characterization of nanocrystalline materials has been conducted. However, there are only a few experimental tensile studies of nanocrystalline metals with a grain size equal or less than 25nm [1-4]. One reason for the scarcity of results is the difficulty in processing pure and defect free materials. Electrodeposition has proven to be a versatile technique to fabricate metallic nanostructures [5]. The grain size of electrodeposits depends on the deposition parameters such as pH of the electrolyte [6], deposition technique [2], current density [7], and substrate [8], as well as on the type and the amount of additives included in the electrolyte [9]. One other method that seems to effectively reduce the grain size of the electrodeposits to very small sizes (<25nm) is alloying. The electrodeposition of Ni-Fe alloys has been investigated by several researchers [10-13] and has been shown that the composition and the grain size of the deposits can be varied by controlling the deposition parameters as well as the electrolyte composition. Ni and Fe are completely soluble in each other; however there are ordering tendencies near Ni-25 at% Fe (Ni_3Fe) and Ni-75% Fe ($NiFe_3$) compositions. The crystal structure of nickel-rich alloys is FCC (face centered cubic) and the iron-rich alloys have BCC (body centered cubic) structures. Among the FCC Ni-Fe alloys, the Ni-20 wt% Fe, known as Permalloy, has applications in the electromagnetic devices. In this study, the properties of electrodeposited FCC Ni-Fe alloys with the composition in the range 5 to 50 wt% Fe have been investigated.

2. EXPERIMENTAL PROCEDURES

The electrolyte used in this study was composed of 1.2M nickel sulfamate, 0.5M boric acid, 2gl^{-1} L-asorbic acid and 0.5gl^{-1} SNAP (sulfamate nickel anti-pit). The iron was added as either $FeCl_2.4H_2O$ or $FeSO_4.7H_2O$ salt. The amount of iron in the deposit was varied by changing the Ni/Fe ion ratio. The pH of the electrolyte was kept at 2.00 by adding a few drops of sulfuric acid and it was deareated immediately before deposition by blowing nitrogen gas for approximately 45 minutes. The deposition was conducted at a bath temperature of 25 °C.

The deposition cell consisted of a conventional rotating disc. The details of the deposition setup can be found elsewhere [14,15]. The cathode rotation speed was 500 rpm for all deposits. The deposition was conducted galvanostatically at the cur-

Corresponding author: F. Ebrahimi, e-mail: e-mail: febra@mse.ufl.edu

Table 1. Summary of the properties of the Ni-Fe deposits fabricated in this study.

Deposit #	1	2	3	4	5	6	7	8	9	10
$FeCl_2 \cdot 4H_2O$ (M)	0.075	0.03	0.03		0.01				0.005	
$FeSO_4 \cdot 7H_2O$ (M)				0.03		0.007	0.007	0.005		0.0015
Fe (wt%)	51	42.7	42.3	35	25.5	21	21.2	14.9	14.8	5.6
Grain size (nm), XRD	11	11	10	10.5	10.8	14	10.5	10.4	10.3	-
Grain size (nm), TEM	-	-	-	-	-	11.3 (4.7)**	9.1 (5)	8.8 (4.7)	-	60.6 (80)
$I_{(200)}/I_{(111)}$*	0.39	0.25	0.19	0.41	0.24	0.21	0.28	0.25	0.28	14.3

* The standard ratio for random distribution of Ni_3Fe particles is 0.59.
** Values in the parentheses are the standard deviations.

rent density of 25 $mAcm^{-2}$. The deposition time varied among the deposits and resulted in thickness values in the range of 20 to 50μm. The substrate, which was removed chemically after deposition, was a 35 mm-diameter disc of annealed copper with a strong (100) rolling plane texture.

The composition of the deposits was measured by the electron microprobe analysis using the JEOL superprobe 733 system. The lattice parameter, lattice strain, crystallographic texture and the approximate average grain size were characterized using the x-ray diffraction (XRD) technique. A Philips APD 3720 system and the accompanied software were used for XRD analysis. The (111) peak was used for analysis, except for the alloy with the lowest iron content, which showed a strong <100> texture. For this alloy the (200) peak was analyzed. The microstructure and the grain size of selected deposits were evaluated using the transmission electron microscopy (TEM) technique. The grain size was measured using the dark field TEM images taken at high magnifications. At least 200 grains per sample were examined. The size of each grain was estimated by calculating the average of the longest length and the length perpendicular to it. The strength of the freestanding deposits was evaluated by microhardness testing using a Buehler Micromet II system. The applied load was 10g or 25g, depending on the strength level, and the loading time was 15s. The average hardness was calculated from applying at least ten indents.

3. RESULTS

The variations in grain size and texture with the iron content of the deposits are shown in Table 1. The texture and the grain size were nominally the same in alloys with 15 to 50 wt% Fe. These deposits showed a very fine grain size with an average size of approximately 11nm. There is a reasonable agreement between the average grain sizes obtained by the XRD technique and those calculated from the TEM images. The standard deviations associated with the latter measurements were relatively small, suggesting that these deposits had a tight grain size distribution. When the iron content of the deposit was reduced to 5.6 %, the grain size increased drastically and so did the standard deviation. Parallel to the drastic change in the grain size, there was a dramatic modification of the texture. While the high iron content alloys showed a near random texture with a slight <111> tendency, the deposit with 5.6 % Fe exhibited a strong <100> texture as indicated by the high $I_{(200)}/I_{(111)}$ ratio.

Fig. 1 presents variations of lattice parameter, lattice strain and microhardness as a function of the iron content of the deposits. Both the lattice parameter and lattice strain increased with the iron content of the deposits. The internal stresses developed in the high iron content deposits were significant enough to cause noticeable curvature in the deposits. Indeed alloys with more than 35 wt% Fe developed microcracks as shown in Fig. 2.

The hardness as a function of the iron content is presented in Fig. 1c. The hardness increased initially, exhibited a maximum around 15 to 20 % iron and then decreased with increasing the iron content. The hardness measured for the Ni-20 wt% Fe deposit is comparable to the hardness reported for the electrodeposited Permalloy with 12nm grain size [11].

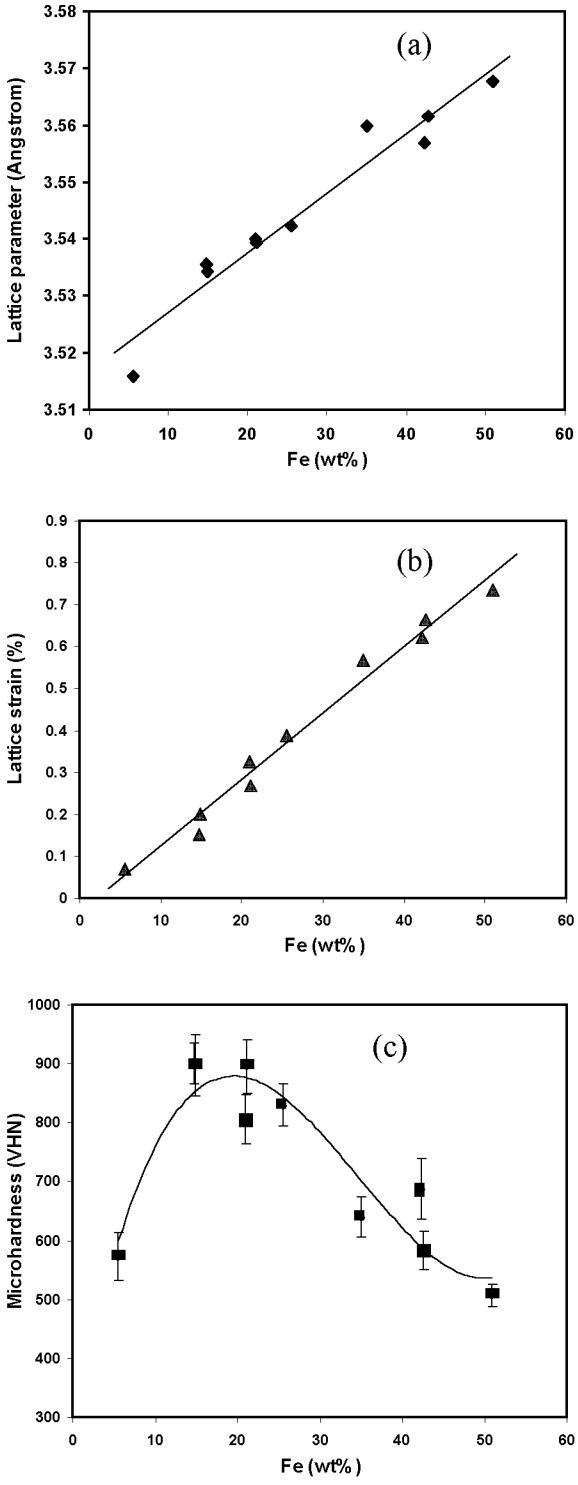

Fig 1. Variations in (a) lattice parameter, (b) lattice strain and (c) Vickers microhardness of the deposits as a function of the iron content.

Electrodeposits usually have a high concentration of defects, such as vacancies, dislocations, twins, stacking faults and voids. Fig. 3 gives a high resolution TEM micrograph of Ni-21 % Fe deposit showing the fine grain size and the presence of twin

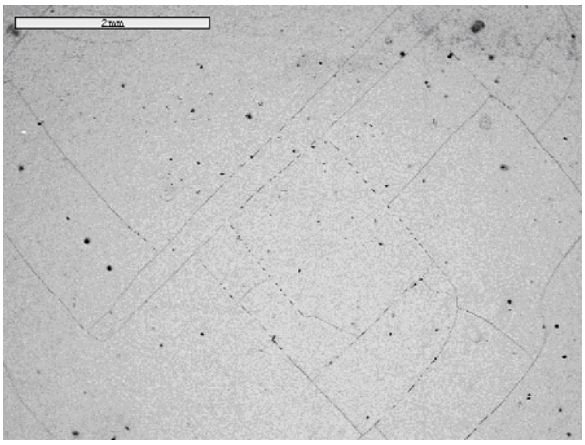

Fig. 2. SEM micrograph showing the formation of microcracks in the Ni-42.7% deposit.

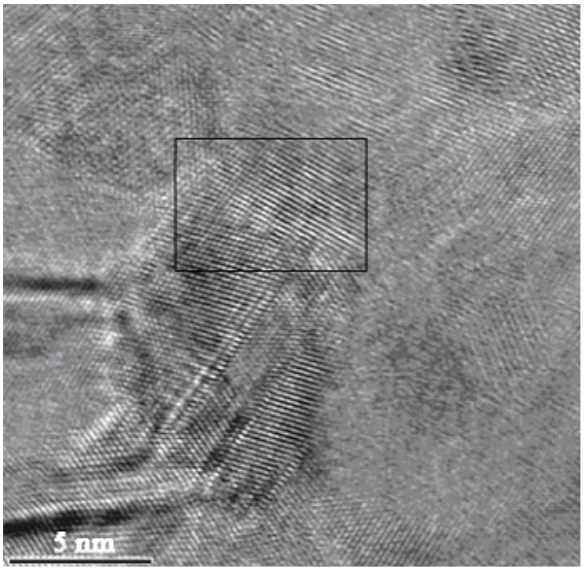

Fig. 3. High resolution TEM picture of the Ni-21 wt% Fe deposit showing the fine grain size, presence of twin and low angle boundaries. The area that contains the low angle boundary is boxed. Note the presence of dislocations at this boundary.

and low angle boundaries. Consistent with the previously reported studies [1], no amorphous region was found near the high angle boundaries and the lattice images remained sharp within atomic distance from these boundaries.

4. DISCUSSION

The increase in the lattice parameter with increasing the iron content of the nanocrystalline deposits found in this study is consistent with the behavior observed in conventional well annealed and electrodeposited FCC Ni-Fe alloys [13]. However, the values measured here are slightly lower than those

reported for the well annealed alloys. Due to the development of residual lattice strains in the deposits, this difference may be attributed to the presence of the internal compressive stresses along the crystallographic directions whose peaks were used to calculate the lattice parameter.

The XRD results confirmed that all the deposits had the FCC crystal structure. Because nickel and iron are 100% soluble and are expected to have FCC structure in the composition range investigated here, the observed increase in the lattice strain cannot be attributed to the super-saturation of alloys or the presence of non-equilibrium phases. Furthermore, there is no correlation between the reduction in grain size and the increase in the internal stresses. The former remained constant while the latter value increased continuously with increasing the iron concentration. Several theories have been proposed to explain the development of internal stresses in electrodeposits [16]. It has been suggested that the level of internal stresses in Ni-Fe electrodeposits is due to the lattice mismatch between the deposit and the substrate [16]. However, the copper substrate used in this study has a larger lattice parameter (lattice parameter of Cu = 3.6150 Angstrom) than the Ni-Fe alloys do. Raising the iron content increases the lattice parameter of the alloy and brings it closer to that of copper, and hence should decrease rather than increase the level of internal strains. Also, because the current efficiency and the deposition potential do not considerably depend on the iron concentration of the bath [12], the theories based on the hydrogen evolution do not apply. Therefore, it is suggested that the increase in the lattice strain and the associated microcracking tendency with increasing the iron concentration is due to an increase in the defect content of the deposits. It should be noted that contrary to the solidification process, there is little relaxation in the bulk of electrodeposits because of the low processing temperature. Any rearrangement of atoms occurs at the deposit/electrolyte interface, and consequently surface diffusion plays an important role on the development of defects in electrodeposits. Should an increase in the iron concentration of the electrolyte reduce the surface diffusion, more defective structure with higher internal stresses is expected to develop in deposits with higher iron contents.

The results of this study show that the grain size of the Ni-Fe deposits is independent of the iron content in the 15 wt% to 50 wt% compositional range. This is contrary to the results reported for Ni-Fe deposits fabricated from a sulfate bath with saccharin additive in a quiescent bath [17]. The two important factors that affect the nucleation rate during electrodeposition are overpotential and presence of additives [18]. The latter effect is not relevant to this study because no additives were used. Also, at a constant current density and rotation speed, no significant variation in the overpotential with the ferrous content of the electrolyte is predicted [12]. Therefore, in this study no change in the grain size with the iron content of the deposits is expected.

It has been shown that during the co-deposition of nickel and iron, the deposition of iron is enhanced and the reduction of nickel is inhibited when compared to their individual deposition rates. This effect has been attributed to a faster adsorption of the $Fe(OH)^{+1}$ ion in comparison to the $Ni(OH)^{+1}$ ion on the cathode surface [12]. However, at low iron to nickel ion ratios, the reduction of nickel becomes the dominant controlling mechanism. The grain size of nickel deposits in the absence of iron is strongly dependent on the pH of the bath and there is an optimum pH value where the finest grain size is obtained [6]. It is suggested that the combination of low pH (pH = 2) and the low concentration of iron (0.0015M of $FeSO_4.7H_2O$) resulted in the relatively large grain size of the alloy with 5.6 wt% Fe. In sulfamate-based solutions, nickel deposits tends to grow along the <100> direction. We have shown that the larger the grain size the stronger is the crystallographic texture [2,3,6-8]. Therefore, the <100> texture observed in the Ni-5.6 wt% Fe alloy is attributed to its large grain size.

The results for coarse-grained conventional FCC Ni-Fe alloys indicate that the strength of these alloys is not sensitive to the iron content [15,17], therefore classical solid solution hardening cannot explain the variation of hardness with the iron content observed in this study. The hardening due to the increase in the iron content from 5.6 wt% to approximately 15 wt% Fe can be attributed to the reduction in the grain size. However, the hardness for pure nickel with approximately 11nm grain size is reported to be 650 VHN [19], which suggests that the grain size change may not be sufficient for explaining the increase in hardness. On the other hand, the deposits with equal or larger than approximately 15 wt% Fe have relatively similar grain sizes and their slight variations cannot explain the reduction in the hardness with increasing the iron concentration. Several factors may contribute to the variation in hardness including ordering near the Ni_3Fe composition [15], presence of internal stresses and the

width of the grain size distribution [3]. Further work is needed to investigate the composition dependency of the strength of nanocrystalline Ni-Fe alloys.

4. CONCLUSIONS

The results of this study led to the following conclusions regarding the properties of electrodeposited nanocrystalline Ni-Fe alloys with iron content in the range of 15 to 50 wt%.

(a) Consistent with the behavior of well annealed alloys, the lattice parameter of the deposits increased with increasing the iron content.
(b) Grain size decreased drastically when the iron content of the deposit was increased from 5.7 wt% to 15 wt%. This change is attributed to the dominance of the Fe deposition at the higher ferrous bath content.
(c) In spite of the constancy of the average grain size, hardness decreased and the level of internal stresses increased with increasing the iron content above 15 wt%. This behavior may be associated with an increase in the defect structure of the deposits.

REFERENCES

[1] J. R. Weertman, D. Farkas , K. Hemker , H. Kung, M. Mayo, R. Mitra and H. Van Swygenhoven // *MRS Bull.* **24** (1999) 44.
[2] K. L. Morgan, Z. Ahmed, and F. Ebrahimi // *MRS Proceedings* **634** (2001) B.3.11.1.
[3] F. Ebrahimi, Z. Ahmed and K. L. Morgan // *MRS Proceedings* **634** (2001) B.2.7.1.
[4] F. Dalla Torre, H. Van Swygenhoven and M. Victoria // *Acta Mater.* **50** (2002) 3957.
[5] F. Ebrahimi, D. Kong, T. E. Matthews and Q. Zhai, In: *Processing and Fabrication of Advanced Materials VII*, ed. by Srivastan and Khor (TMS Publication: Warrendale, PA, 1998) p.509.
[6] F. Ebrahimi, G. R. Bourne, M. S. Kelly and T. E. Matthews // *NanoStructured Materials* **11** (1999) 343.
[7] F. Ebrahimi and Z. Ahmed // *Journ. Appl. Electrochem,* in press 2003.
[8] F. Ebrahimi and Z. Ahmed // *Materials Characterization* **49** (2003) 373.
[9] A. M. El-Sherrik and U. Erb // *Mater. Sci. Eng.* **30** (1995) 5743.
[10] D. L. Grimmett, M. Schwartz and K. Nobe // *J. Electrochem. Soc.* **140** (1993) 973.
[11] C. Cheung, G. Plaumbo and U. Erb // *Scripta Metall. Mater.* **31** (1994) 735.
[12] K. –M. Yin and C.-C. Lee // *J. Chem. Tech. Biotechno.* **70** (1997) 337.
[13] S. D. Lieth, S. Ramli and D. T. Schwartz // *J. Electrochem. Soc.* **146** (1999) 1431.
[14] F. Ebrahimi, Q. Zhai and D. Kong // *Mater. Sci. Eng.* **255** (1998) 20.
[15] H. Li and F. Ebrahimi // *Mater. Sci Eng.* **347** (2003) 93.
[16] S. E. Hadian and D. R. Gabe // *Surface and Coating Tech* **122** (1999) 118.
[17] C. Cheung, F. Djuanda, U. Erb and G. Plalumbo // *NanoStructured Materials* **5** (1995) 513.
[18] F. C. Walsh and M. E. Herron // *J. Applied Physics* **24** (1991) 217.
[19] U. Erb // *NanoStructured Materials* **6** (1995) 533.